The Continuous Harmonic-Tuned Power Amplifier

Brian M. Merrick, *Student Member, IEEE*, Justin B. King, *Member, IEEE*, and Thomas J. Brazil, *Fellow*, *IEEE*

***Abstract*—In this work, a new power amplifier (PA) mode is introduced – the continuous Harmonic-Tuned 2nd (HT_2) mode. The mode offers the potential to deliver high efficiency across wide bandwidths. The voltage and current waveforms required to realise this novel mode are examined, theoretical performance is described, and measurement results are presented, verifying the theory.**

***Index Terms*—High efficiency, power amplifiers (PAs).**

I. Introduction

THE continuous expansion of mobile communications networks has led to an ever-increasing demand for PAs capable of delivering high efficiencies across multiple wide, and possibly non-contiguous, bandwidths. With future standards expected to place even more stringent requirements on the wireless front-end, this demand is set to increase.

It has long been known that manipulating the harmonic impedances presented at the transistor current-generator plane can give a large improvement in amplifier performance by allowing for an increase in the fundamental voltage (or current) component beyond that of the traditional, conduction angle-dependent, or "tuned-load", modes of operation, such as Class-B [1]. By adding a third harmonic component to the voltage waveform, for example, we arrive at Class-F. In [2], the HT_2, or "Class-G", PA mode was proposed, which utilises a second harmonic drain voltage component to greatly increase the allowable fundamental voltage while ensuring the $i_{\mathrm{ds}} - v_{\mathrm{ds}}$ loadline avoids the knee region of the drain characteristic. This work was further expanded upon in [3], in which the Harmonic-Tuned 2nd, 3rd ($HT_{2,3}$), or "Class-FG", mode was described, further improving theoretical amplifier performance. More recently, the "Saturated Amplifier" was introduced [4], [5], which exploits the nonlinear output capacitance to generate desirable voltage and current waveforms.

Concurrently, the continuous modes of amplifier operation were introduced [6], which greatly increased the allowable operating bandwidth of the traditional high efficiency PAs, for example, the continuous Class-F PA mode [7].

In this work, the continuous HT_2 mode is presented. In Section II, the theory behind the HT PA is introduced, and the continuous voltage waveforms are described. In Section III, the generation of the required harmonic voltage is discussed. In Section IV, measurement and simulation results are presented. Finally, in Section V, conclusions are drawn.

II. Harmonic-Tuned Amplifier Theory

The addition of suitably-phased harmonic components to the voltage waveform at the current-generator plane has the effect of increasing the peak of the waveform while flattening the trough, thereby allowing an increase in the fundamental load and a corresponding increase in efficiency. Such a voltage waveform, normalised to the drain dc voltage, can be written as

$$v_{\mathrm{ds}}(\theta) = 1 - v_1 \left(\cos(\theta) + \sum_{n=2}^{\infty} k_n \cos(n\theta) \right), \qquad (1)$$

where v_1 is the normalised-to-dc fundamental voltage component and k_n is the voltage ratio between the n^{th} harmonic and the fundamental.

From [2], the optimum values for v_1 and k_2 (i.e. the values that maximise the amplitude of the fundamental while avoiding zero-crossing) lead to the following equation for the HT_2 voltage waveform:

$$v_{\mathrm{HT}_2}(\theta) = 1 - \sqrt{2}\cos(\theta) + \frac{1}{2}\cos(2\theta). \qquad (2)$$

Equation (2) suggests an efficiency improvement of $41\,\%$ for the HT_2 mode PA when compared with the tuned-load amplifier. This would seemingly imply efficiencies greater than $100\,\%$ for certain conduction angle values. Section III will describe the actual efficiency improvement deliverable by this mode.

When the term $(1 - \gamma \sin(\theta))$ [6] is applied to (2), we get the following expressions for the continuous HT_2 PA mode:

$$\begin{aligned} v_{\mathrm{HT}_2}(\theta,\gamma) \;=\;& 1 - \sqrt{2}\cos(\theta) - \frac{3\gamma}{4}\sin(\theta) + \frac{1}{2}\cos(2\theta) \\ &+ \frac{\gamma}{\sqrt{2}}\sin(2\theta) - \frac{\gamma}{4}\sin(3\theta), \end{aligned} \qquad (3)$$

with the parameter $\gamma \in [-1, 1]$ differentiating between the different waveforms in the HT_2 continuum. For completeness, we note that the $HT_{2,3}$ mode can be similarly expanded, giving the continuous $HT_{2,3}$ PA mode:

$$\begin{aligned} v_{\mathrm{HT}_{2,3}}(\theta,\gamma) \;=\;& 1 - 1.62\cos(\theta) - 0.555\gamma\sin(\theta) \\ &+ 0.891\cos(2\theta) + 0.673\gamma\sin(2\theta) \\ &- 0.275\cos(3\theta) - 0.446\gamma\sin(3\theta) \\ &+ 0.138\gamma\sin(4\theta). \end{aligned} \qquad (4)$$

As is always the case for continuous modes, higher harmonics must be taken into account than with the traditional amplifier modes. It should also be noted that the waveform of (3) is the same as that theorised and experimentally verified in [8] and [9], respectively, for the continuous Class-F^{-1} mode, as the waveform in question is a practical approximation of the ideal half-wave sinusoid of the theoretical Class-F^{-1}. However, in the continuous Class F^{-1} mode, the current waveform is assumed to be a square wave, whereas in this work the current waveform will range from strongly bifurcated to near-sinusoidal, depending on the chosen bias point. The continuous HT_2 mode voltage waveforms are shown in Fig. 1.

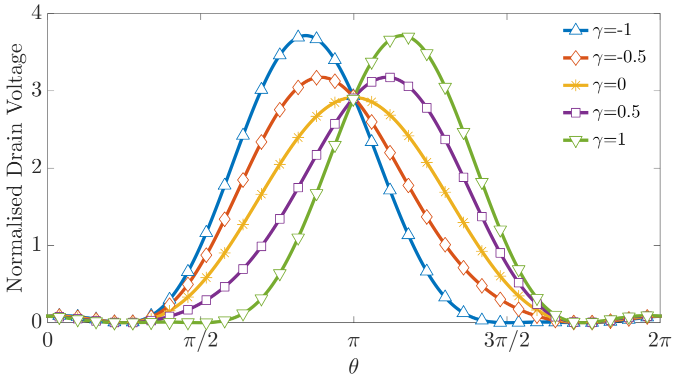

Fig. 1. The continuous HT_2 mode voltage waveforms.

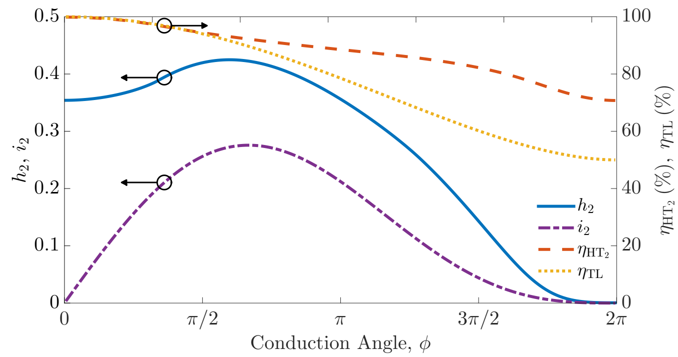

Fig. 2. h_2 (blue, solid), i_2 for the tuned-load case (purple, dash-dotted), HT_2 mode drain efficiency (red, dashed), and tuned-load drain efficiency (yellow, dotted), versus conduction angle, ϕ. In order for the mode to be realisable by passive means, i_2 must be reduced below zero.

III. Harmonic Voltage Generation

From (2), we can see that the fundamental and second harmonic voltage components are in antiphase with one another. Assuming a standard, conduction-angle-dependent current waveform, an impedance with a negative real part is required at the second harmonic due to the fundamental and second harmonic current components being in-phase [1]. In order to be able to realise a HT_2 mode PA using passive matching networks, amplifier nonlinearities can be exploited to generate the required voltage (it is also possible to use an external amplifier to generate the desired phase relationship i.e. through active load-pull of the device [10]). Both the input nonlinear capacitance, C_{gs}, and the output nonlinear capacitance, C_{out} (incorporating both C_{ds} and C_{gd} through the Miller effect), have been proposed as possible means of generating the desired voltage waveform.

A. Input nonlinearity generation

In [2], it was demonstrated that it is feasible to exploit C_{gs} to generate a second harmonic voltage at the gate so as to appropriately flatten the voltage waveform. Provided the amplitude of this second harmonic component is sufficiently large relative to the fundamental, the phase of the second harmonic current component of i_{ds} will be inverted and the amplifier output matching network will be realisable by conventional passive means. This will also have the effect of increasing the conduction angle from that of the standard tuned-load. Following the terminology of [1], we define h_2 as the ratio between the second harmonic and fundamental voltage components. Fig. 2 plots the minimum magnitude of h_2 required to invert the second harmonic phase versus the conduction angle, ϕ, of the amplifier, as well as the associated drain efficiency for this waveform. For reference, the drain efficiency and second harmonic current component of the tuned-load amplifier are also shown. As can be seen, a large improvement in efficiency can be achieved for a wide range of ϕ. The potential efficiency improvement of 41 % given by the increased fundamental drain voltage is only achieved for higher values of ϕ, as the previously mentioned increase in the effective conduction angle will result in an increase in the DC component of the drain current, reducing efficiency.

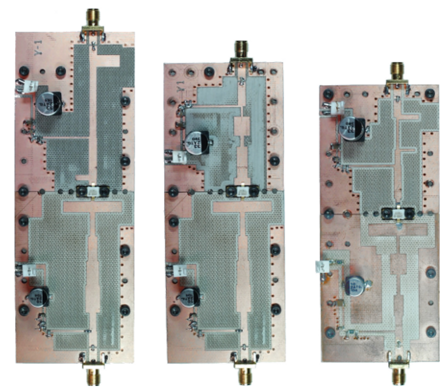

(a) $\gamma = -1$ (b) $\gamma = 1$ (c) AB

Fig. 3. The realised HT_2 and Class-AB PAs.

B. Output nonlinearity generation

The Saturated Amplifier concept suggests a different route to achieving high efficiency. If the second harmonic impedance presented in parallel with C_{out} is sufficiently large, and the amplifier is driven into saturation, then C_{out} will dominate harmonic wave-shaping, and an appropriately-phased second harmonic voltage will be generated. This in turn allows the fundamental impedance magnitude to be increased, improving efficiency.

In practice, both the input and output capacitive nonlinearities will likely contribute to some degree to the generation of the desired waveforms, and, provided they are correctly generated, their method of generation is somewhat irrelevant to the PA designer.

IV. Experimental Verification

In order to verify the theory presented above, two prototype HT_2 PAs, representing $\gamma = \pm 1$, as well as a comparison Class-AB PA, were designed for operation at 2.14 GHz using Cree CGH40010 10 W GaN HEMTs, thus demonstrating the expanded design space for broadband PAs provided by this mode. The realised PAs are shown in Fig. 3, and their schematics are given in Fig. 4. All three were fabricated using Taconic RF-35 with relative permittivity $\epsilon_r = 3.5$, a height of 1.52 mm, and a copper thickness of 70 µm. Due to the inability to access the intrinsic gate voltage waveform, it was

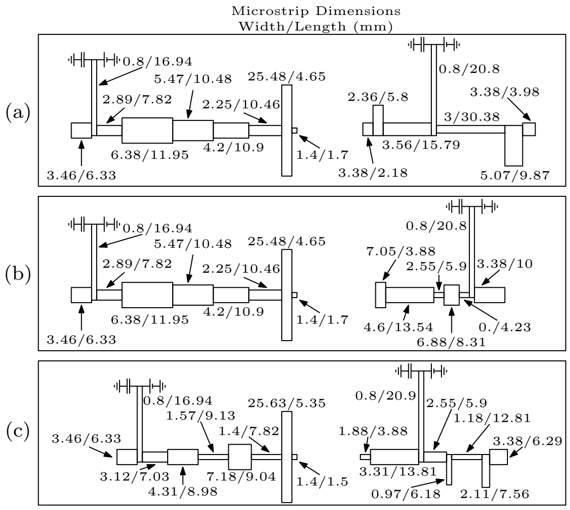

Fig. 4. Schematics for the three realised PAs: (a) $\gamma = -1$, (b) $\gamma = 1$, (c) Class-AB.

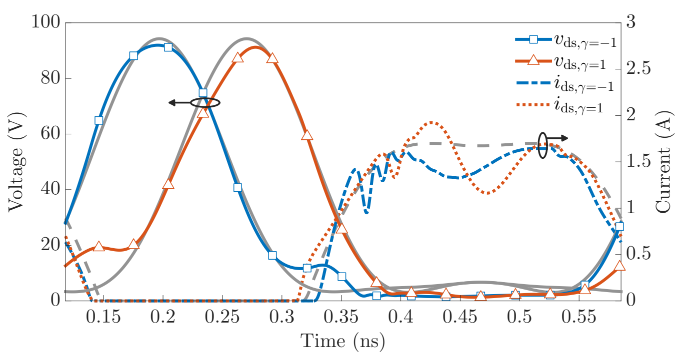

Fig. 5. Simulations using the full, nonlinear, manufacturer-supplied model. Shown are the current-generator plane voltage (solid, markers) and current (dashed) waveforms of the realised PAs, for $\gamma = -1$ (blue) and $\gamma = 1$ (red). For comparison, the theoretical voltage and current waveforms are shown in grey, demonstrating excellent adherence to the theory.

not possible to ascertain whether input or output nonlinearities were responsible for the required second harmonic voltage generation. The PAs were biased at a quiescent drain current of 370 mA, corresponding to a current angle of approximately 1.2π radians, with the impedances chosen such that the second harmonic current phase has been just inverted ($Z_2 \approx \infty$). Fig. 5 shows the simulated current-generator plane voltage and current waveforms of the two prototypes, as well as those of theoretical HT_2 PAs with $V_{\mathrm{DS}} = 28\,\mathrm{V}$, $V_{\mathrm{knee}} = 4\,\mathrm{V}$, and $I_{\mathrm{peak}} = 1.7\,\mathrm{A}$. The simulations were undertaken using a nonlinear model supplied by Cree. As can be seen, excellent agreement is achieved between the theoretical and simulated waveforms. Measurements of the PAs confirmed this agreement with theory, as shown in Table I. Also shown in Table I are the measurement results of the fabricated Class-AB PA, demonstrating the large efficiency and power boost conferred by the HT_2 design strategy. Available input power was approximately 25 dBm for these measurements. Discrepancies between the measured and theoretical results may be attributed to model inaccuracies, in addition to the required theoretical impedances not being exactly met.

TABLE I
COMPARISON OF THEORETICAL AND MEASURED RESULTS.

	Theory		Measurement		
	$\mathrm{HT}_{2,\mathrm{theory}}$	$\mathrm{AB}_{\mathrm{theory}}$	$\mathrm{HT}_{2,\gamma=-1}$	$\mathrm{HT}_{2,\gamma=1}$	AB
η (%)	74.3	60	67.3	70.3	53.2
P_{out} (dBm)	42.4	40.3	42.7	42.15	40.5
Gain (dB)	–	–	18.2	17.7	15.5

V. CONCLUSIONS

In this work, the continuous HT_2 mode PA was introduced. Its theoretical voltage waveforms were described, and its improved performance over tuned-load PAs discussed. In order to verify the theory, two prototype continuous HT_2 PAs were designed, with each giving large improvements in power and efficiency over their equivalent Class-AB PA. Finally, the simulated waveforms of the designed PAs were examined, demonstrating excellent agreement with the presented theory. In conclusion, the continuous HT_2 mode PA shows excellent promise for further expanding the available design space for high efficiency and wide bandwidth PAs.

REFERENCES

[1] P. Colantonio, F. Giannini, and E. Limiti, *High Efficiency RF and Microwave Solid State Power Amplifiers*. John Wiley & Sons, Ltd, 2009.

[2] P. Colantonio, F. Giannini, G. Leuzzi, and E. Limiti, “High efficiency low-voltage power amplifier design by second-harmonic manipulation,” *Int. J. RF Microw. C. E.*, vol. 10, no. 1, pp. 19–32, 2000.

[3] P. Colantonio, F. Giannini, G. Leuzzi, and E. Limiti, “Multiharmonic manipulation for highly efficient microwave power amplifiers,” *Int. J. RF Microw. C. E.*, vol. 11, no. 6, pp. 366–384, 2001.

[4] J. Kim, J. Moon, B. Kim, and R. Pengelly, “A saturated PA with high efficiency,” *IEEE Microw. Mag.*, vol. 10, pp. 126–133, February 2009.

[5] J. Kim, J. Kim, J. Moon, J. Son, I. Kim, S. Jee, and B. Kim, “Saturated power amplifier optimized for efficiency using self-generated harmonic current and voltage,” *IEEE Trans. Microw. Theory Tech.*, vol. 59, pp. 2049–2058, Aug 2011.

[6] S. Cripps, P. Tasker, A. Clarke, J. Lees, and J. Benedikt, “On the continuity of high efficiency modes in linear RF power amplifiers,” *IEEE Microw. Wireless Compon. Lett.*, vol. 19, pp. 665–667, Oct 2009.

[7] V. Carrubba, A. L. Clarke, M. Akmal, J. Lees, J. Benedikt, P. J. Tasker, and S. C. Cripps, “The continuous class-F mode power amplifier,” in *Proc. Eur. Microw. Integr. Circuits Conf. (EuMIC)*, pp. 432–435, 2010.

[8] C. Friesicke and A. Jacob, “Mode continua for inverse class-F RF power amplifiers,” in *Microwave Conference (GeMIC), 2011 German*, pp. 1 –4, march 2011.

[9] V. Carrubba, J. Bell, R. Smith, M. Akmal, Z. Yusoff, J. Lees, J. Benedikt, P. Tasker, and S. Cripps, “Inverse class-FJ: Experimental validation of a new PA voltage waveform family,” in *Microwave Conference Proceedings (APMC), 2011 Asia-Pacific*, pp. 1254 –1257, dec. 2011.

[10] M. Seo, H. Lee, J. Gu, H. Kim, J. Ham, W. Choi, Y. Yun, K. Kenneth, and Y. Yang, “High-efficiency power amplifier using an active second-harmonic injection technique under optimized third-harmonic termination,” *IEEE Trans. Circuits Syst. II, Exp. Briefs*, vol. 61, pp. 549–553, Aug 2014.